16th ICAAR LISBOA 2020-2022
16th International Conference on
Alkali-Aggregate Reaction in Concrete
Lisboa | LNEC | Portugal | 31 May - 2 June 2022
http://icaar2020-2022.lnec.pt

Investigation of alkali silica reaction damage by acoustic emission and damage rating index methods

S. Tayfur (1), C. Yuksel (2), O. Akar (3), N. Alver (4), O. Andic-Cakir (5)

(1) Department of Civil Engineering, Faculty of Engineering, Ege University, Izmir, Turkey, sena.tayfur@ege.edu.tr

(2) Department of Civil Engineering, Faculty of Engineering, Ege University, Izmir, Turkey, cihat.yuksel@ege.edu.tr

(3) Department of Material Science and Engineering, Graduate Faculty of Natural and Applied Science, Ege University, Izmir, Turkey, ousakr35@gmail.com

(4) Department of Civil Engineering, Faculty of Engineering, Ege University, Izmir, Turkey, ninel.alver@ege.edu.tr

(5) Department of Civil Engineering, Faculty of Engineering, Ege University, Izmir, Turkey, ozge.andic@ege.edu.tr

Abstract

Alkali silica reaction (ASR) which occurs between alkalis in cement and some types of aggregates having reactive components is considered as a serious durability problem. ASR is a detrimental reaction which leads to expansion and damage in hardened concrete. ASR seems to be influenced by numerous factors such as pore solution alkalinity, concrete permeability, grain size distribution of aggregate, alkali gradients in structure and presence of moisture. ASR shows itself in the form of map-like cracking, joint closure due to expansion, gel leakage and particle fragmentation in structural members. The most common and effective way to rate the severity of this damage is imaging and microstructural analysis on core samples drilled from the structures. Besides, non-destructive testing (NDT) methods can help to monitor the consequences of ASR without harming the structure.

In this study, acoustic emission (AE) technique, which is defined as transient elastic wave release due to local fractures in a stressed material, was used for monitoring ASR damage in concrete. AE is one of the most effective NDT tools to identify location, size and severity of the cracks. Accordingly, accelerated concrete prism test was conducted on three concrete mixtures with different levels of reactivity, damage rating index (DRI) -a microscopic and semi-quantitative petrographic tool- and AE measurements were made simultaneously. Consequently, expansion data, AE results and DRI values were compared and correlations between these methods were determined. It was observed that AE is an effective tool for monitoring ASR damage. Particularly, the AE energy released during crack formations seems to correlate well with both expansion and DRI data.

***Keywords**: accelerated concrete prism test; acoustic emission (AE); alkali silica reaction (ASR); damage rating index (DRI)*

1. INTRODUCTION

The most common method of determining the potential alkali-silica reactivity is preparing mortar/concrete prisms in laboratory environment, exposing them to accelerated test conditions and making periodic expansion measurements. Petrographic investigations on samples contribute significantly to understand the possible underlying factors affecting the reaction and its exact mechanism. Since the early research by Grattan-Bellew and Danay in 1992 [1], Damage Rating Index (DRI) method has become a valuable tool for detecting and quantifying the deterioration resulting from ASR. This semi-quantitative petrographic method is based on counting the number of different damage features on polished sections, multiplying them by assigned weighing factors which are related to their relative importance and finding a final DRI value which provides some guidance for comparatively interpreting the data [2, 3]. Meanwhile, non-destructive testing has become an important and even essential tool in structural health monitoring applications. Among non-destructive tests, acoustic emission (AE) can give valuable information about the dynamic degradation process occurring within the concrete elements since it detects the generation and growth of cracks and thus the damage degree.

AE is defined in [4] as “the class of phenomena whereby transient elastic waves are generated by the rapid release of energy from localized sources within a material”. The elastic waves are detected by piezoelectric sensors placed on the surface, are converted into electrical signals and analysed. Thus, it is an important non-destructive testing method which ensures that the material tested is checked for reliability and structural integrity [5]. Purpose of an AE monitoring system is to detect signals from AE sources, to record their amounts and distributions in relation to one or more test variables such as load, pressure, temperature, and to classify and localize them. The method is frequently used for monitoring damage processes in concrete or any materials such as crack and delamination of strengthening materials, leakages in pipelines and high-pressure vessels. Studies on application of AE tests for investigating the durability-related problems of reinforced concrete are mostly limited to detection of corrosion process [6-8].

Utilization of AE for monitoring ASR damages is rarely seen in the literature and there are deficiencies in application of the technique. Abdelrahman et al [9] concluded that AE could detect ASR damages, by correlating AE activities with ASR degradation. Farnam et al [10] used AE and X-ray computed tomography analysis to detect cracks due to ASR and investigated frequency ranges of AE activities due to cracks generated in the matrix or aggregates. Lokajíček et al [11] evaluated the early stages of the reaction by developing semi-continuous ultrasound determination and AE monitoring system in mortar specimens exposed to ASR. Accelerated concrete prism test was not applied in any of these studies. The aim of this study was to investigate the efficiency of AE monitoring by correlating the findings obtained with ASR expansions of the similar mixtures, as well as correlating these with the damage measured by DRI method.

2. MATERIALS AND METHODS

2.1 Materials

CEM I 42.5 R type portland cement (complying with EN 197-1) with an equivalent Na_2O content of 1.15% was used as binder. Its chemical composition is presented in Table 2.1.

Table 2.1: Chemical composition of the cement (wt%)

	SiO_2	Al_2O_3	Fe_2O_3	CaO	MgO	SO_3	Na_2O	K_2O	LOI[a]
Cement	18.60	5.59	3.04	61.47	1.32	3.26	0.62	0.81	3.75

[a]Loss on Ignition

Three aggregate types representing different reactivity levels were selected for the experimental study. These aggregates, in decreasing order of reactivity, can be listed as waste glass cullet, a type of andesitic basalt (with a glassy matrix of ~70% SiO_2) and a non-reactive limestone aggregate. According to our previous experience, the potential expansion produced by glass, basalt and limestone aggregates after performing accelerated mortar bar (80°C, 1 N NaOH solution) test correspond to 1.16%, 0.52% and 0.01%, respectively. It should be emphasized that this classification of reactivity was made according to RILEM AAR-2 [12] test; however, RILEM AAR-4.1 [13] procedure (accelerated concrete prism test) was followed in the current experimental study. Basalt and limestone aggregates were used in 0/4, 4/16 and 11.2/22.4 mm size fractions; meanwhile, glass was used as fine aggregate only.

2.2 Concrete mixtures

In order to investigate the reactivity levels of concrete mixtures including the above-mentioned aggregates, three mixtures were prepared. These mixtures had a cement content of 440 kg/m^3 and water/cement ratio of 0.5. Coarse to fine aggregate ratio was 60:40 by mass.

The mixtures abbreviated as BST and LMS include only basalt and limestone aggregates, respectively. The alkali contents of these mixtures were boosted to 1.25% Na_2O equivalent by adding NaOH pellets to the mixing water. Additionally, a highly reactive mixture labelled as GLS was cast by using glass as fine aggregate and basalt as coarse aggregate. Alkali boosting was not applied in this mixture. Details on mixture proportions can be seen in Table 2.2.

Table 2.2: Amounts of ingredients in each mixture

	Mixture proportions (kg/m^3)		
	BST	GLS	LMS
Cement	440	440	440
Water	220	220	220
0/4 basalt	699	-	-
4/16 basalt	524	500	-
11.2/22.4 basalt	524	500	-
0/4 waste glass	-	665	-
0/4 limestone	-	-	652
4/16 limestone	-	-	660
11.2/22.4 limestone	-	-	334
NaOH	0.58	-	0.58

2.3 Expansion measurements

75x75x285 mm prisms cast from each mixture were demoulded 24 h after casting, initial length measurements were made and they were transferred to the storage containers containing water at their bottom part. Then, they were stored at 60°C in a reactor type cabinet for 20 weeks in accordance with AAR-4.1. Length readings were taken at regular intervals after cooling down the prisms inside their containers for 16±4 hours at 20°C.

2.4 AE setup

8-channel Micro SAMOS AE System by Mistras Holding was used for AE measurements. One piezoelectric AE sensor with resonance frequency of 150 kHz was attached by silicon grease on each test specimen (Figure 2.1a) and 42 dB threshold was set to eliminate ambient noise. In order to prevent damage to the sensors in this high-temperature and high-humidity environment, they were covered with plastic containers and silicone before they were placed in 60°C cabinet (Figure 2.1b-c). The sensors were calibrated with the Hsu-Nielsen Calibration Method (Figure 2.1d). Afterwards, test was started up and data was recorded continuously (approximately 120 days).

Recorded AE activities were evaluated by time-based parameter analysis. The main signal parameters used were amount of activity, amplitude, energy and cumulative energy (Figure 2.2). Amount of AE activity is a crucial parameter indicating the amount of damage. Amplitude -the maximum voltage reached in the signal- is directly related to the magnitude of the damage. Energy also gives an idea about the energy and scale of the damage.

2.5 DRI testing

DRI method is performed by examining the polished sections under a stereobinocular microscope, plotting grids of 1 cm x 1 cm on the samples and counting the number of features associated with ASR damage. Then, the count of each feature is multiplied with an assigned weighing factor indicating its importance in overall damage process. The total number is normalized for an area of 100 cm^2 and reported as DRI value. Types of deterioration features and the weighing factors assigned for each one were taken from the original method proposed in 1992 [1]. Since then, many researchers used DRI method for assessing ASR and modifications to weighing factors were suggested in some of the studies [14, 15].

In this study, a revised version of the method was applied. In order to perform DRI testing, first, 15 mm thick slices were cut from 75x75x285 mm prisms. After that, vacuum fluorescent epoxy impregnated and polished samples were prepared. Sections were scanned under stereomicroscope at 16x magnification. For this purpose, surfaces were first sub-divided into smaller regions of interest and then, each captured image was merged into one. Concerned damage features and application of weighing factors were based on the study of Grattan-Bellew [2] which is summarized in Table 2.3; however, counting the number of gels in aggregate or cement paste was excluded due to resolution limitations. DRI was assessed on specimens exposed to 60°C at the same time intervals as expansion readings were made.

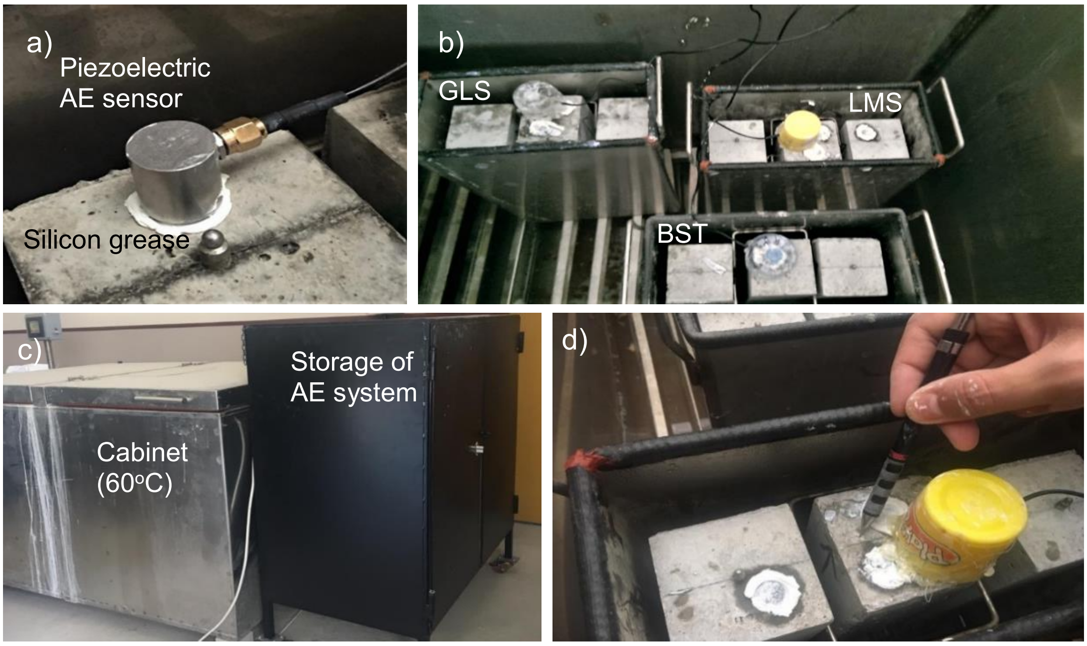

Figure 2.1: AE test setup: a) placement of piezoelectric AE sensor, b) test specimens in 60°C-cabinet, c) general view of test setup, d) calibration of the AE sensors by Hsu-Nielsen method

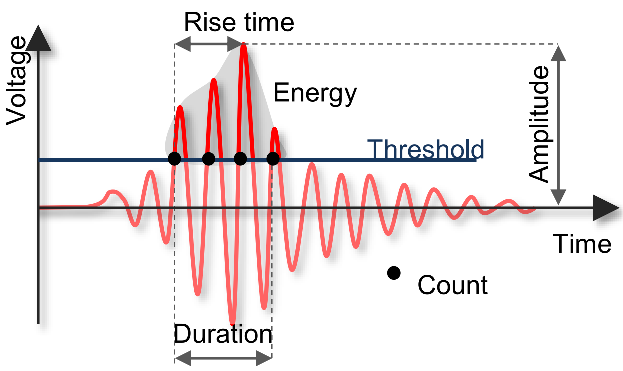

Figure 2.2: AE signal parameters

Table 2.3: Weighing factors used for DRI assessment [2]

Damage feature	Assigned weighing factor
Coarse aggregate with crack	x0.25
Coarse aggregate with open crack	x3
Coarse aggregate with cracks and gel	x2
Coarse aggregate debonded	x3
Coarse aggregate with reaction rim	x0.5
Cement paste with cracks	x2
Cement paste with cracks and gel	x4
Air void with gel	x0.5

3. RESULTS AND DISCUSSION

The expansion-time plots of each mixture are shown in Figure 3.1a. The mixture incorporating glass as fine aggregate expanded far more than the other mixtures at each age. This mixture expanded very rapidly within the first 7 weeks. Afterwards, despite the reduction in rate of expansion increase, a continuous rise in expansion values was observed throughout the entire testing period. Expansion of BST mixture did not exceed the RILEM recommended limit (0.03%) in accelerated concrete prism test. Nonetheless, it showed higher length change values compared to LMS mixture. While 20-week expansion value of GLS mixture reached 0.426%, the corresponding values for BST and LMS mixtures were 0.023% and 0.009%, respectively.

According to the DRI results given in Figure 3.1b, the greater degree of expansion in GLS mixture resulted in greater DRI values among all mixtures. The number of counts in GLS mixture increased up to 15 weeks with the highest rate of DRI increase occurring between the 5th and 15th weeks of exposure. At 5th week, the main feature was the reaction rims observed in some coarse aggregate particles. With increasing exposure duration, the counts falling into this category did not show a significant variation. The main feature of deterioration in GLS mixture after this period was the “cracks in cement paste” since its amount was found to rise continuously and significantly up to 15 weeks. This may result from the fact that very highly reactive glass particles were used as fine aggregate in this study and the reaction sites originating from these small-sized particles are viewed as dispersed in cement matrix. Similarly, the most observed features in BST mixtures were reaction rims and cement paste cracks. Particularly, the number of cement paste cracks and thus, calculated DRI values in this mixture remained lower than those found in GLS mixture. Both in GLS and BST mixtures the numbers of closed/open cracks within the aggregate remained considerably low. The non-expansive character of LMS mixture was also reflected in DRI testing. Except the cracks which were probably present due to crushing operations applied to limestone aggregate before being used in concrete, almost no damage feature was observed in LMS mixture.

Interestingly, a drop was observed in DRI values between the ages of 15th and 20th weeks. A possible explanation for this behaviour might be the closure of some cracks with the crystallized products of reaction at later ages leading to some reduction in DRI values. Considering the small number of samples (3 sections for each DRI value in this study) and high variation between the results in some cases, this subject requires further testing. Since the expansion limit recommended by RILEM is based on the 15th week measurements, expansion and DRI values observed up to this age will be used to try to correlate test parameters in the following parts.

Figure 3.2 shows some examples of section parts viewed by plain and ultraviolet light to count damage features.

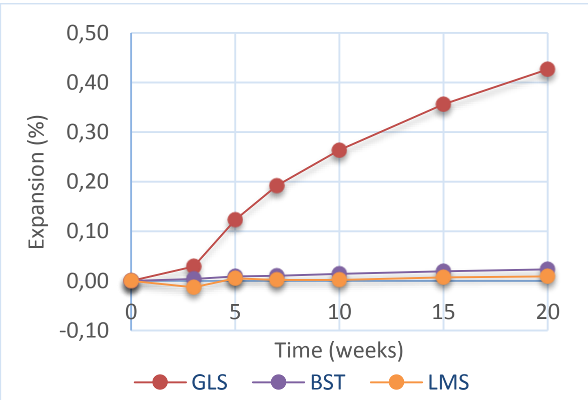

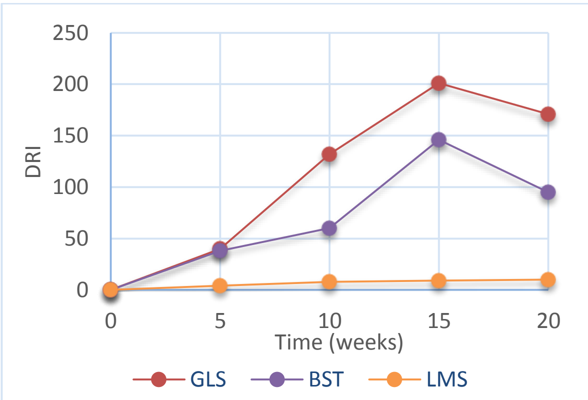

Figure 3.1: Expansion-time and DRI-time plots for each mixtures

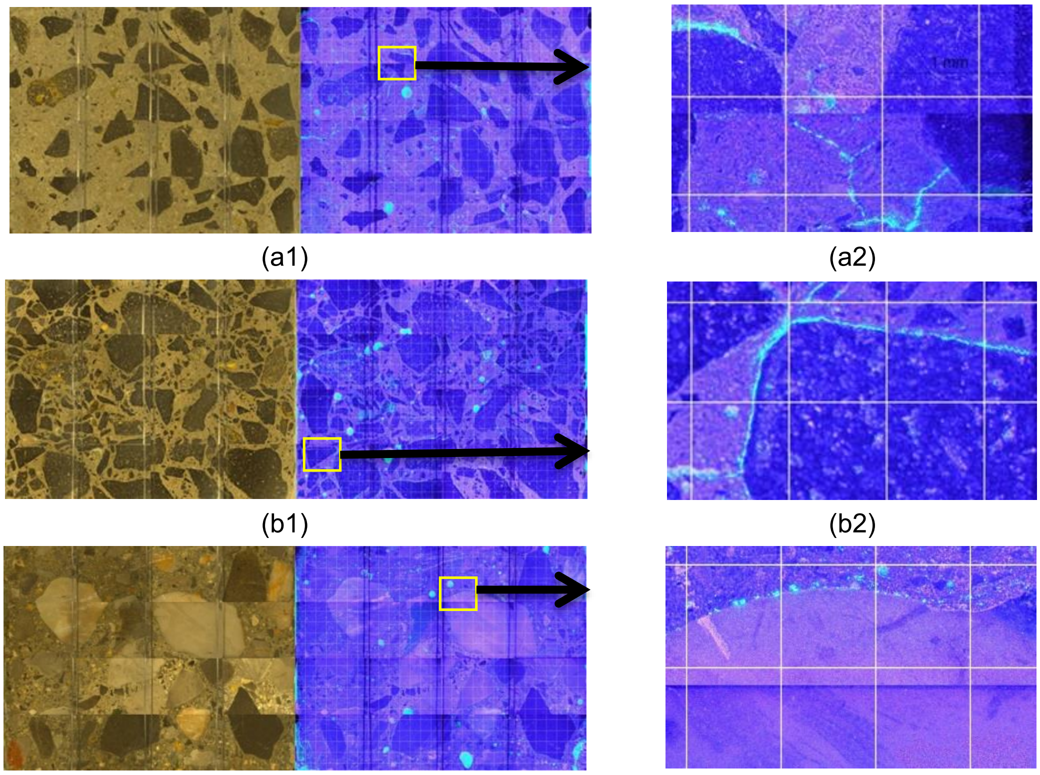

Figure 3.2: Plain-light and ultraviolet-light images obtained for a) GLS, b) BST and c) LMS mixtures at 15th week of testing

AE data obtained from the tests were analysed by time-based parameter analyses. As it can be clearly seen from Figure 3.3, both AE activities and their energies of GLS are higher than those of the other specimens. Moreover, although lower amount of AE activities were observed in BST, its cumulative AE energy is higher than that of LMS. Thus, much more and micro-scale damages originated in LMS.

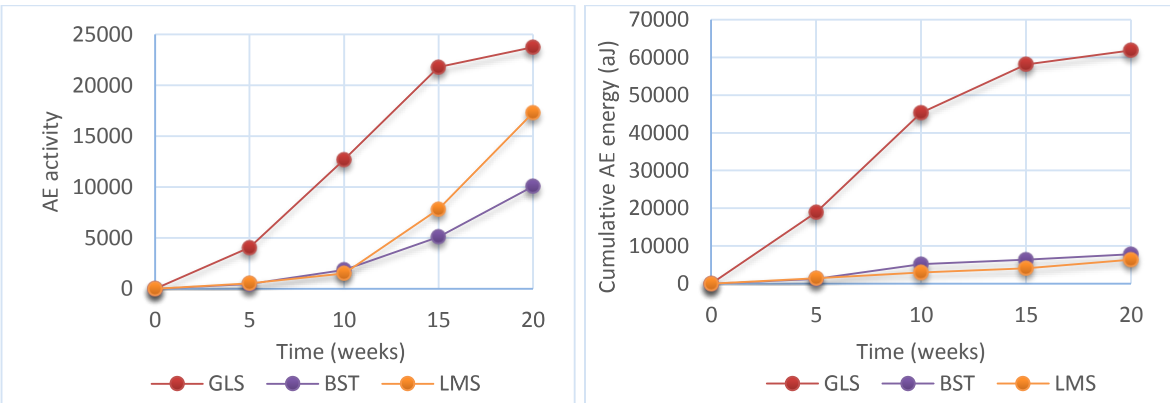

Figure 3.3: Parameter-based AE analysis results of the specimens

Figure 3.4 presents expansion/DRI measurements vs. AE (amount and energy) relationships of the mixtures. As the specimens damaged, both expansion and DRI values as well as AE parameters increased. As expected, the most expansion was measured in GLS. Therefore, the highest number of AE activities was also counted in this mixture. On the other hand, although BST expanded more, its AE activities were less than those of LMS.

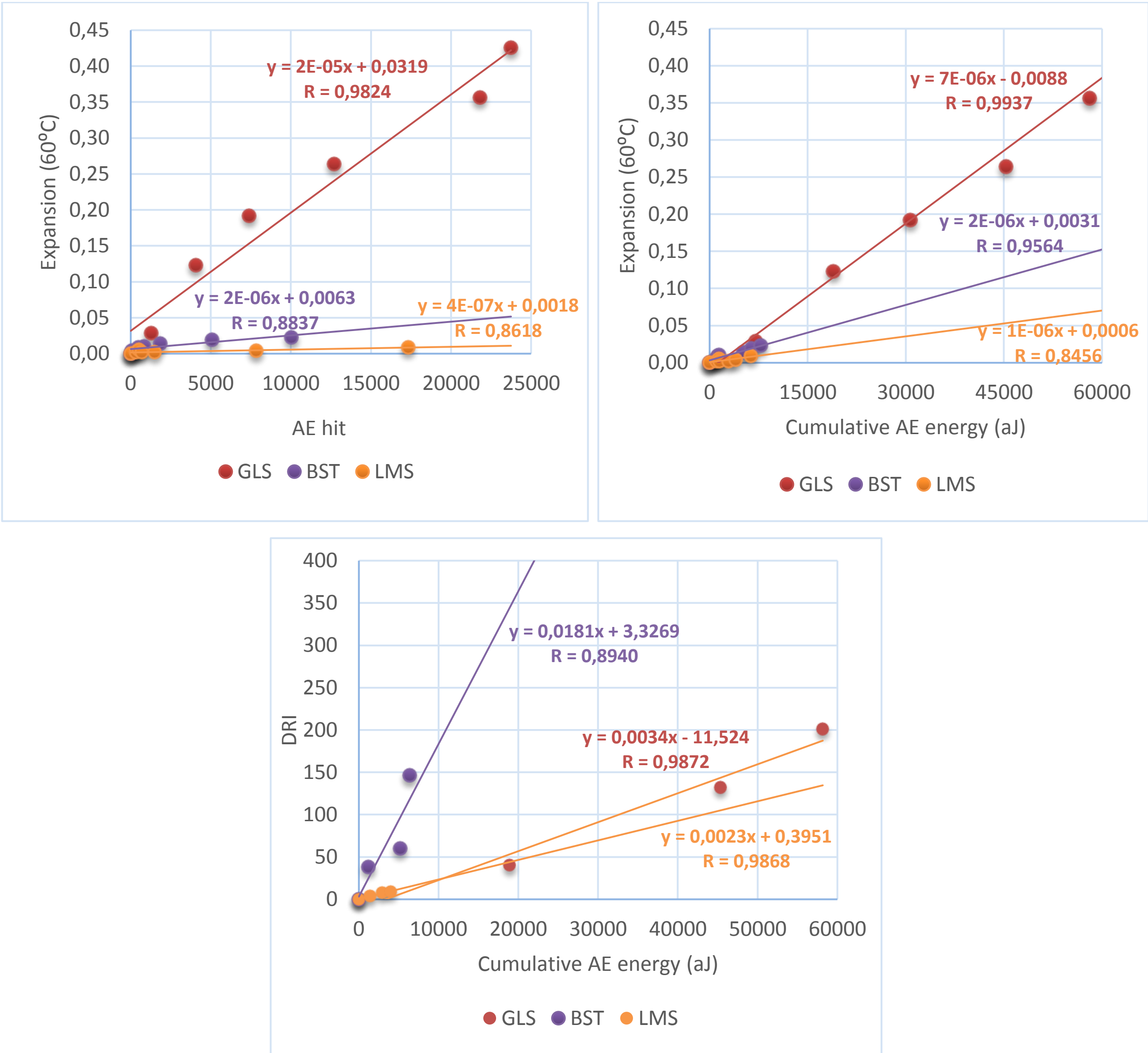

Figure 3.4: AE hit vs. expansion, cumulative AE energy vs. expansion and cumulative AE energy vs. DRI relationships of the mixtures

Considering the relationship between expansion and cumulative AE energy, differences in damage formations of the mixtures can be understood. The cumulative AE energy in decreasing order was GLS (61852 aJ), BST (7811 aJ) and LMS (6347 aJ), respectively. The highest cumulative AE energy was formed in the GLS mixture which is the most reactive mixture. Therefore, the scale and number of cracks occurred in GLS mixture was the most among the ones tested. On the other hand, although the amount of AE activity in BST is less than LMS, opposite situations was seen in AE energies. This means that fewer but more macro-sized cracks occurred in BST. Therefore, it was more damaged than LMS.

According to regression equations and correlation coefficients of the distributions, the strongest relationship was obtained from GLS mixture for both expansion vs. AE hit and expansion vs. cumulative AE energy, respectively. On the other hand, the relationships mentioned in BST and LMS mixture are weaker than GLS, but they are at acceptable levels. Nonetheless, it is not reasonable to try to create correlations for non-reactive mixtures since expansion, DRI and AE energy values of LMS vary in very small ranges. The correlation coefficients found for GLS and BST mixtures in expansion-energy plots were higher than those found in expansion-hit graphs. This seems logical since the extent of expansion is related not only to the amount of generated cracks but also to the width/length of them.

Finally, when the cumulative AE energy vs. DRI relationships are evaluated, the difference between DRI values of GLS and BST is less compared to the difference between the released AE energies. This state again indicates that GLS damaged more. In addition, the strongest relationship for AE energy vs. DRI was also obtained from GLS.

4. CONCLUSION

In this study, ASR occurrence and damage were investigated in concrete prisms prepared from three mixtures having different reactivity potentials. In addition to the classical concrete prism tests, damage progressions were monitored by the non-destructive testing method "AE" and the semi-quantitative "DRI" method. Following conclusions were obtained from the study:

- Expansion of glass bearing GLS mixture reached extremely high values at each age compared to other mixtures. Basalt bearing BST mixture expanded more than non-reactive limestone bearing LMS, but the expansion value did not exceed the critical limit in accelerated concrete prism test.
- According to DRI measurements, GLS mixture had the highest number of damage features. The main feature type for this mixture was "cracks in cement paste". Most common categories of features observed in BST were "reaction rims" and "cracks in cement paste".
- It was observed that AE is an effective method for monitoring ASR damage and AE parameters are effective characteristics in evaluating such damages.
- The ranking between the cumulative AE energy values released in the mixtures is the same as the order of the expansion (GLS>BST>LMS).
- Both the number of AE activities and high AE energy values of GLS are directly related to the number of cracks and the extent of the damage.
- The strongest relationships between both AE activities vs. expansion and cumulative AE energy vs. expansion were obtained from GLS. It is thought that the relationship between cumulative AE energy vs. expansion is more meaningful because it includes the extent of the damage.

ACKNOWLEDGEMENT

The authors would like to thank The Scientific and Technical Research Council of Turkey (TUBITAK) for the financial support provided under Project: 118M240.

REFERENCES

[1] Grattan-Bellew PE, Danay A (1992) Comparison of laboratory and field evaluation of AAR in large dams. Proc. of the International Conference on Concrete AAR in Hydroelectric Plants and Dams. Canadian Electrical Association & Canadian National Committee of the Int. Commission on Large Dams. Fredericton New Brunswick, Canada.

[2] Grattan-Bellew PE (2012) Petrographic methods for distinguishing between alkali-silica, alkali-carbonate reactions and other mechanisms of concrete deterioration. 14th ICAAR – International Conference on Alkali-Aggregate Reaction in Concrete. May 20-25, Austin, Texas.

[3] Sanchez LFM, Fournier B, Jolin M, Duchesne J (2015) Reliable quantification of AAR damage through assessment of the damage rating index (DRI). Cem Concr Res 67:74-92. https://doi.org/10.1016/j.cemconres.2014.08.002

[4] Terminology S (2004) Nondestructive Examinations 1. Policy 03:1–40. https://doi.org/10.1520/E1316-19.Radiologic

[5] Sun L, Li Y, Li C, et al (2010) Active defects detection and localization using acoustic emission method. Proc World Congr Intell Control Autom 5348–5351. https://doi.org/10.1109/WCICA.2010.5554798

[6] Kawasaki Y, Wakuda T, Kobarai T, Ohtsu M (2013) Corrosion mechanisms in reinforced concrete by acoustic emission. Cons Build Mat 48:1240-1247. https://doi.org/10.1016/j.conbuildmat.2013.02.020

[7] Idrissi H, Limam A (2003) Study and characterization by acoustic emission and electrochemical measurements of concrete deterioration caused by reinforcement steel corrosion. NDT & E Int 36:563-569. https://doi.org/10.1016/S0963-8695(03)00064-1

[8] Van Steen C, Pahlavan L, Wevers M, Verstrynge (2019) Localisation and characterisation of corrosion damage in reinforced concrete by means of acoustic emission and X-ray computed tomography. Cons Build Mat 197:21-29. https://doi.org/10.1016/j.conbuildmat.2018.11.159

[9] Abdelrahman M, ElBatanouny MK, Ziehl P, et al (2015) Classification of alkali-silica reaction damage using acoustic emission: A proof-of-concept study. Cons Build Mat 95:406–413. https://doi.org/10.1016/j.conbuildmat.2015.07.093

[10] Farnam Y, Geiker MR, Bentz D, Weiss J (2015) Acoustic emission waveform characterization of crack origin and mode in fractured and ASR damaged concrete. Cem Concr Compos 60:135–145. https://doi.org/10.1016/j.cemconcomp.2015.04.008

[11] Lokajíček T, Přikryl R, Šachlová Š, Kuchařová A (2017) Acoustic emission monitoring of crack formation during alkali silica reactivity accelerated mortar bar test. Eng Geol 220:175–182. https://doi.org/10.1016/j.enggeo.2017.02.009

[12] RILEM AAR-2 (2016) Detection of Potential Alkali-Reactivity – Accelerated Mortar-Bar Test Method for Aggregates. In: Nixon PJ and Sims I (eds.). RILEM Recommendations for the Prevention of Damage by Alkali-Aggregate Reactions in New Concrete Structures State-of-the-Art Report of the RILEM Technical Committee 219-ACS. Springer. 61-77.

[13] RILEM AAR-4.1 (2016) Detection of Potential Alkali-Reactivity – 60°C Test Method for Aggregate Combinations Using Concrete Prisms. In: Nixon PJ and Sims I (eds.). RILEM Recommendations for the Prevention of Damage by Alkali-Aggregate Reactions in New Concrete Structures State-of-the-Art Report of the RILEM Technical Committee 219-ACS. Springer. 99-116.

[14] Grattan-Bellew PE, Mitchell LD (2006) Quantitative petrographic analysis of concrete – the damage rating index (DRI) method, a review. In Marc-André Bérubé Symp. on Alkali-aggregate reactivity in concrete. Montréal, Canada, p. 321-334.

[15] Villeneuve V, Fournier B, Duchesne J (2012) Determination of the damage in concrete affected by ASR – the damage rating index (DRI). 14th ICAAR – International Conference on Alkali-Aggregate Reaction in Concrete. May 20-25, Austin, Texas.